Unique Backbone-Water Interaction Detected in Sphingomyelin Bilayers with $^{1}H/^{31}P$ and $^{1}H/^{13}C$ HETCOR MAS NMR Spectroscopy

Gregory P. Holland* and Todd M. Alam†
*Magnetic Resonance Research Center, Department of Chemistry and Biochemistry, Arizona State University, Tempe, Arizona; and †Department of Nanostructured and Electronic Materials, Sandia National Laboratories, Albuquerque, New Mexico

ABSTRACT Two-dimensional $^{1}H/^{31}P$ dipolar heteronuclear correlation (HETCOR) magic-angle spinning nuclear magnetic resonance (NMR) is used to investigate the correlation of the lipid headgroup with various intra- and intermolecular proton environments. Cross-polarization NMR techniques involving ^{31}P have not been previously pursued to a great extent in lipid bilayers due to the long ^{1}H-^{31}P distances and high degree of headgroup mobility that averages the dipolar coupling in the liquid crystalline phase. The results presented herein show that this approach is very promising and yields information not readily available with other experimental methods. Of particular interest is the detection of a unique lipid backbone-water intermolecular interaction in egg sphingomyelin (SM) that is not observed in lipids with glycerol backbones like phosphatidylcholines. This backbone-water interaction in SM is probed when a mixing period allowing magnetization exchange between different ^{1}H environments via the nuclear Overhauser effect (NOE) is included in the NMR pulse sequence. The molecular information provided by these $^{1}H/^{31}P$ dipolar HETCOR experiments with NOE mixing differ from those previously obtained by conventional NOE spectroscopy and heteronuclear NOE spectroscopy NMR experiments. In addition, two-dimensional $^{1}H/^{13}C$ INEPT HETCOR experiments with NOE mixing support the $^{1}H/^{31}P$ dipolar HETCOR results and confirm the presence of a H_2O environment that has nonvanishing dipolar interactions with the SM backbone.

INTRODUCTION

Sphingomyelin (SM) and phosphatidylcholine (PC) comprise the majority of eukaryotic cell membranes (1). Sphingomyelin is particularly interesting because of its role in the formation of lipid rafts (2). Lipid rafts are believed to be responsible for a number of cellular processes including signal transduction, protein sorting, and cholesterol shuttling (2–6). These rafts are liquid-ordered domains of saturated chain phospholipids and cholesterol. These domains laterally phase-separate from liquid-disordered phospholipids and have been linked to a number of diseases including HIV and Alzheimer's (7–12). There is increasing evidence that cholesterol prefers to interact with saturated chain sphingolipids over saturated chain glycerophospholipids of similar chain lengths (13). There are only two main structural differences between these two classes of lipids: 1), the sphingosine backbone in sphingolipids compared to the glycerol backbone in the glycerophospholipids; and 2), the *trans* double bond between the C4 and C5 carbon of the acyl chain in sphingolipids (see structure in Fig. 2) compared to no double bond in glycerophospholipids (see structure in Fig. 4). The presence of the double bond in sphingolipids is thought to be responsible for the tighter acyl-chain packing and thus, higher chain order parameter observed for sphingolipids over glycerophospholipids (14,15).

The unique role of SM in membrane function and the formation of raft phases could be due to the sphingosine backbone. The sphingosine backbone has both hydrogen-bond acceptors (the amide group and carbonyl group) and a hydrogen-bond donor (the hydroxyl group) while the glycerol backbone of PC contains only hydrogen-bond acceptors (the carbonyl groups). This unique backbone of SM permits participation in both intra- and intermolecular hydrogen-bonding interactions. The formation of a possible hydrogen-bonded network at the interfacial region of sphingomyelin may explain a more favorable interaction with cholesterol by shielding it from interactions with water. This is similar to the previously proposed Umbrella model where the main requirement for cholesterol incorporation in a lipid bilayer is the phospholipid headgroup's ability to cover the hydrophobic cholesterol molecules from interactions with water (16–18). This model was used to explain the cholesterol solubility limits in different lipids including why PC with its larger headgroup can incorporate more cholesterol than the smaller headgroups of phosphatidylethanolamine (16). Water could potentially be involved in this hydrogen-bonded network at the SM interface and the possibility of intermolecular hydrogen-bonded water bridges between neighboring SM molecules in bilayers has been proposed (19). Unfortunately, experimental evidence that supports the existence of this hydrogen-bonded network in SM bilayers and the involvement of water at the sphingosine backbone is limited. Infrared and Raman spectroscopies have been used to investigate the role of inter- and intramolecular bonds in SM; unfortunately, the results are inconclusive with respect to assignments in the amide I and amide II bands (20,21). High resolution ^{1}H and ^{31}P nuclear magnetic resonance (NMR) have argued for an intramolecular hydrogen bond between

Submitted January 30, 2008, and accepted for publication March 7, 2008.

Address reprint requests to Gregory P. Holland, Tel.: 480-965-7915; E-mail: greg.holland@asu.edu.

Editor: Anthony Watts.

0006-3495/08/08/1189/10 $2.00

doi: 10.1529/biophysj.108.130724

the SM hydroxyl and the phosphodiester group (19,22), while more recent ^{2}H NMR studies have probed the interfacial polarity and the water/hydroxyl and water/amide exchange rates (23), suggesting that it is the amide residue involved in intermolecular hydrogen bonding.

One-dimensional ^{31}P magic-angle spinning (MAS) NMR techniques have been extensively applied to the study of lipid bilayer systems (24–32) and have been recently utilized to study raft formation in tertiary lipid systems containing cholesterol (33). A few reports on the application of two-dimensional ^{1}H/^{31}P heteronuclear Overhauser effect spectroscopy (HOESY) (26,34) have appeared on PC and phosphatidylethanolamine lipids, although the bulk of ^{31}P nuclear Overhauser effect (NOE) studies are of the one-dimensional variety (35–40). NMR experiments involving ^{1}H/^{13}C cross-polarization (CP) have also been shown to be useful in the study of lipid membrane systems and have been implemented in both one-dimensional (25,41–44) and two-dimensional (45–47) experiments. NMR studies involving ^{31}P CP have not been implemented to a large extent because of the long ^{1}H-^{31}P distances and high degree of headgroup mobility that further averages the dipolar coupling. Only a limited number of lipid reports based on ^{31}P CP have appeared in the literature (48–52). In this article, we present an example of a two-dimensional MAS NMR experiment that utilizes ^{1}H-^{31}P CP and a NOE mixing period. These ^{1}H/^{31}P dipolar heteronuclear correlation (HETCOR) NMR methods are particularly useful for studying intra- and intermolecular interactions in SM by including a NOE mixing period before the CP step in the pulse sequence (see Fig. 1). Of specific interest is the ability to probe interactions at the lipid headgroup and backbone. A unique dipolar network involving strongly associated water is detected at the backbone of SM that is not detected in PC lipids. Further characterization of this intermolecular dipolar proton network was provided by two-dimensional ^{1}H/^{13}C INEPT HETCOR experiments with NOE mixing.

MATERIALS AND METHODS

Materials

Egg sphingomyelin (SM), 1,2-dipalmitoyl-*sn*-glycero-3-phosphocholine (DPPC), 1,2-dimyristoyl-*sn*-glycero-3-phosphocholine (DMPC), and 1,2-dioleoyl-*sn*-glycero-3-phosphocholine (DOPC) were obtained from Avanti Polar Lipids (Alabaster, AL) and used as received. The SM had the following acyl-chain composition: 84% 16:0; 6% 18:0; 2% 20:0; 4% 22:0; and 4% 24:0, and contained no unsaturated acyl chains.

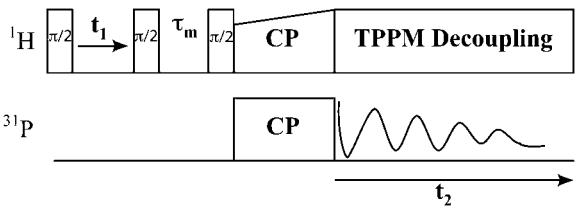

FIGURE 1 Pulse sequence for two-dimensional dipolar HETCOR MAS NMR experiment with NOE mixing period, τ_m.

Sample preparation

Pure lipid samples were prepared by mixing the lipid with deionized water (pH = 7.5) in a conical vial with a vortex mixer. This was followed by a minimum of five freeze-thaw cycles in dry ice and a warm water bath set to 333 K (above the liquid crystalline phase transition for all lipids). Buffer was not used in any of the lipid mixtures to prevent multilamellar vesicle (MLV) fragmentation due to freeze-thaw cycling in the presence of salt (53). Thus, the samples in this study are large MLVs $>\sim 1$ μm in diameter. Samples containing multiple lipid constituents were first combined and dissolved in chloroform followed by vacuum drying overnight at room temperature to remove the solvent. The samples were then hydrated with the above procedure. All lipid samples were 33 wt % phospholipid. The lipid samples were transferred to 4 mm zirconia MAS rotors and sealed with kel-F inserts and caps. The typical volume of MLV sample for NMR analysis was 50–100 μL corresponding to 25–50 mg of phospholipid. The samples were stored in a -20°C freezer when NMR experiments were not being performed.

NMR spectroscopy

NMR spectra were collected on an Avance 600 spectrometer (Bruker Biospin, Billerica, MA) equipped with a 4-mm broadband double-resonance MAS probe spinning at 5 kHz. The temperature was set above the liquid crystalline phase transition of the lipid and controlled to ± 0.2 K with a Bruker VT unit. The reported temperature is adjusted to account for heating effects due to MAS and ^{1}H decoupling as described previously (54). The spectra were collected in a two-dimensional HETCOR fashion with ^{1}H$\rightarrow$^{31}P ramped CP. A moderate ^{1}H two-pulse phase modulation (55) decoupling field strength of 22.5 kHz was applied after the CP contact pulse thru acquisition of the free induction decay using a 15° phase shift (55). CP was achieved with a ramped (50$\rightarrow$100%) spin-lock pulse on the ^{1}H channel and a square pulse on the ^{31}P channel (56). The ^{1}H $\pi/2$ pulse length was 4 μs and the RF field strength for CP at 100% power was 62.5 kHz. To monitor ^{1}H magnetization exchange via the NOE, a mixing period, τ_m, was included in the two-dimensional HETCOR pulse sequence (see Fig. 1) as previously described (57). We refer to these two-dimensional NMR experiments as ^{1}H/^{31}P dipolar HETCOR with NOE mixing. Typical acquisition parameters for two-dimensional experiments were 128 scan averages, 128–256 t_1 points, and a 3 s recycle delay. The NOE buildup curves were obtained by normalization to the total observed HETCOR crosspeak intensity. This normalization reduces the effect of spin relaxation during τ_m. The ^{1}H-^{13}C INEPT MAS NMR HETCOR experiments with ^{1}H-^{1}H magnetization exchange were performed as previously detailed (58). For these INEPT experiments, a 10-kHz spinning speed was utilized with the INEPT interpulse delays, i.e., $\Delta_1 = 2.2$ ms and $\Delta_2 = 1.2$ ms, respectively. Additional optimization details are described elsewhere (58).

RESULTS

^{1}H/^{31}P dipolar HETCOR NMR of SM bilayers

The two-dimensional ^{1}H/^{31}P dipolar HETCOR NMR spectra of SM bilayers collected with two distinct ^{1}H-^{1}H NOE mixing periods, τ_m, are displayed in Fig. 2 *A*, $\tau_m = 20$ μs; and Fig. 2 *B*, $\tau_m = 500$ ms. In Fig. 2 *A*, the mixing period can be considered essentially zero and no ^{1}H-^{1}H magnetization exchange via the NOE effect is observed. This is a baseline spectrum where ^{1}H crosspeaks only appear for proton envi-

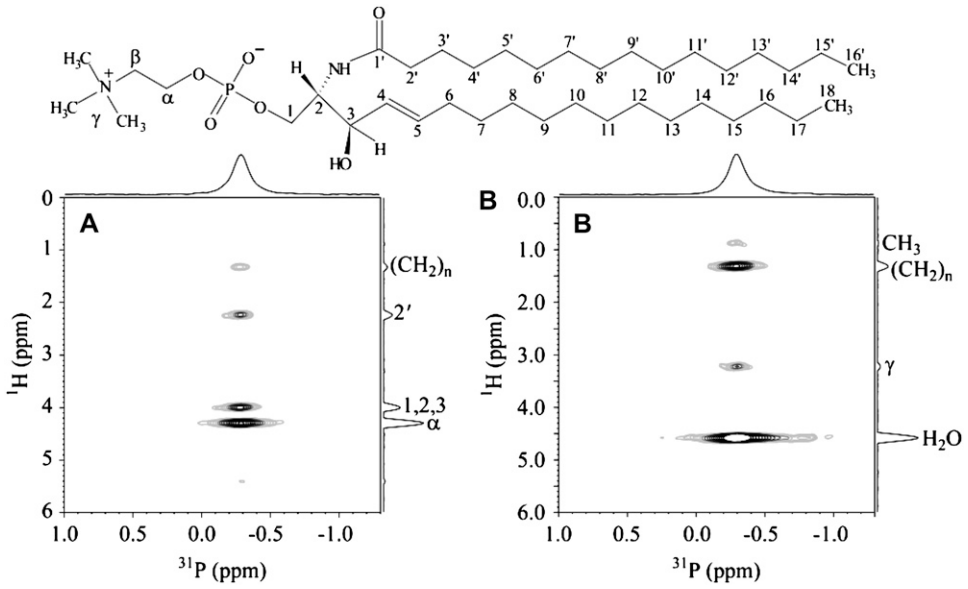

FIGURE 2 The two-dimensional ^{1}H-^{31}P CP dipolar HETCOR MAS NMR spectrum for SM recorded at a sample temperature of 318 K with two different ^{1}H-^{1}H NOE mixing periods; (*A*) τ_m = 20 μs and (*B*) τ_m = 500 ms. The structure of SM with the nomenclature is depicted above the NMR spectra.

ronments that cross-polarize to the ^{31}P nuclei. Up to a 1 ms contact time, strong crosspeaks are observed for the Hα and the SM lipid backbone protons: H1, H2, and H3 (See Fig. 2 for numbering scheme and assignments in SM). The correlation with these different ^{1}H environments is as expected since they are spatially closest to the ^{31}P headgroup and thus, have the strongest dipolar coupling with similar local dynamics. It is assumed that the ^{1}H resonance at $\delta = +4.0$ ppm is dominated by the H1 proton environment due to its close proximity; however, contributions from the H2 and H3 protons cannot be discounted since these three ^{1}H resonances overlap (43,47). Weaker ^{1}H-^{31}P correlations are also observed for the 2′ proton adjacent to the carbonyl and the main chain $(CH_2)_n$ protons. Observation of a correlation peak for the 2′ group is not surprising, considering that orientation of the phospholipid headgroups are essentially perpendicular to the lipid bilayer-normal, positioning the ^{31}P close enough to CP from this proton, particularly if an intramolecular hydrogen bond between the amide proton and the phosphate ester oxygen is considered (59,60). However, the distance between the main chain $(CH_2)_n$ protons and the ^{31}P headgroup is too large for the observed correlation at this contact time to be ascribed to an intramolecular contact. Instead, the ^{1}H-^{31}P correlation involving the $(CH_2)_n$ results from intermolecular contact with adjacent lipid molecules. The observation of unusual intermolecular ^{1}H-^{1}H NOE contacts in phospholipids has been discussed in depth and attributed to the high degree of disorder within the lipid bilayers (61–63). The lack of a CP correlation between H_2O and ^{31}P reveals that there is not a H_2O environment with significant direct ^{1}H-^{31}P dipolar coupling, suggesting that H_2O molecules interacting with the phosphate group are not bound strongly enough to efficiently cross-polarize ^{31}P at these contact times. Contact times as long as 5 ms were attempted with no observation of a H_2O crosspeak. The result shown in Fig. 2 *A* demonstrates that two-dimensional ^{1}H$\rightarrow^{31}$P CP MAS NMR is a powerful tool for studying both intermolecular and intramolecular contacts near the headgroup and backbone of SM.

The two-dimensional ^{1}H-^{31}P dipolar HETCOR MAS NMR spectrum of SM presented in Fig. 2 *B* was collected with a τ_m = 500 ms ^{1}H-^{1}H mixing period to probe proton magnetization exchange via the NOE effect. The observed ^{1}H-^{31}P correlations represent ^{1}H magnetization originally from different proton environments that interact via dipolar cross relaxation with protons involved in the final CP to the ^{31}P nucleus (i.e., the H1, H2, H3, H2′, and Hα proton environments). For this long mixing period the Hα, H1, and the H2′ resonances have completely disappeared. The loss of these Hα, H1, and H2′ correlations results from spin-lattice relaxation and from cross relaxation between these protons and other lipid protons that do not cross-polarize to the ^{31}P headgroup. In these long mixing time experiments (τ_m = 500 ms) several new resonances corresponding to the choline Hγ protons, the terminal methyl CH_3 protons, and H_2O have emerged. It should also be noted that the ^{1}H-^{31}P correlation involving the $(CH_2)_n$ has increased in intensity. Of particular interest is the observation of a strong correlation involving H_2O ($\delta(^1H) = +4.8$ ppm) due to intermolecular contact between H_2O and a proton involved in the final ^{1}H-^{31}P CP step. A stack plot of the indirectly detected ^{1}H spectra as a function of mixing time (τ_m) for SM bilayers provides more insight into this interaction and is depicted in Fig. 3. At mixing times as short as 10 ms, a H_2O resonance is clearly observed indicating a strong ^{1}H-^{1}H magnetization exchange between H_2O and SM. When comparing the ^{1}H spectrum collected with a 1-ms and 10-ms mixing period, the following observations are made: 1), the intensity of Hα decreases by ~8%; 2), the intensity of H1 decreases by ~23%; 3), the $(CH_2)_n$ increases by 52%; 4), H2′ increases by ~11%; and 5), a H_2O resonance is observed that accounts for 13% of the total

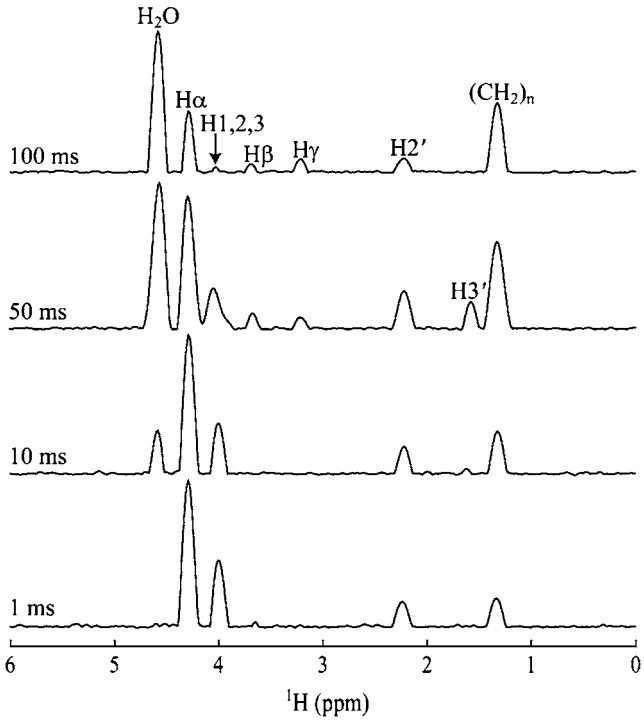

FIGURE 3 The ^{1}H projections from the two-dimensional ^{1}H-^{31}P CP dipolar HETCOR MAS NMR spectra for SM (Fig. 2) at increasing mixing periods' τ_m.

proton crosspeak intensity. Since both Hα and H1 decrease in intensity, these protons participate in dipolar cross relaxation where magnetization is rapidly transferred to the other proton environments. The large increase in intensity of the $(CH_2)_n$ is not due to cross relaxation from H1 or Hα (since the increase is greater than the combined decrease in signal intensity), but is assumed to result from additional magnetization exchange between neighboring $(CH_2)_n$ groups on the chain and protons involved in the final ^{1}H-^{31}P step. The appearance of a strong H_2O resonance with rapid intensity buildup must therefore result from cross relaxation between the H_2O and the Hα and/or H1 environments (involved in the final ^{1}H-^{31}P CP step). This argument is also supported by the observation of the $(CH_2)_n$ correlations being smaller than the H_2O correlations (for $\tau_m > 10$ ms); this precludes a H_2O to $(CH_2)_n$ to backbone proton multistep exchange process. This is also consistent with the faster decrease in the H1,2,3 correlation with increasing mixing time compared to the intensity of the Hα correlation. This result indicates that there is a unique H_2O environment located within the lipid backbone region; however, the observed magnetization exchange process is complicated and quantifying the exact contribution from H1 and Hα to H_2O and/or H2′ is somewhat ambiguous. The ^{1}H/^{13}C INEPT HETCOR NMR with NOE mixing results presented below clarify this problem and show that the H_2O is indeed located at the SM backbone.

^{1}H/^{31}P two-dimensional dipolar HETCOR of DOPC bilayers

The observation of this strong H_2O correlation in the two-dimensional ^{1}H/^{31}P dipolar HETCOR spectra of SM as a function of NOE mixing time prompted the study of other lipid membrane systems. The two-dimensional ^{1}H/^{31}P dipolar HETCOR spectra of DOPC bilayers with a NOE mixing period, $\tau_m = 20$ μs and 500 ms, are shown in Fig. 4, *A* and *B*, respectively. Again, for short mixing times, only correlations between proton environments that cross-polarize and the ^{31}P headgroup are observed. It is interesting to note that all the glycerol backbone protons (g1, g2, and g3), along with the headgroup Hα, and Hγ protons, are observed. The latter is surprising, considering the methyl and phosphorous groups are located six bonds apart, suggesting that instead of an intramolecular interaction that these correlations result from an intermolecular interaction with neighboring DOPC

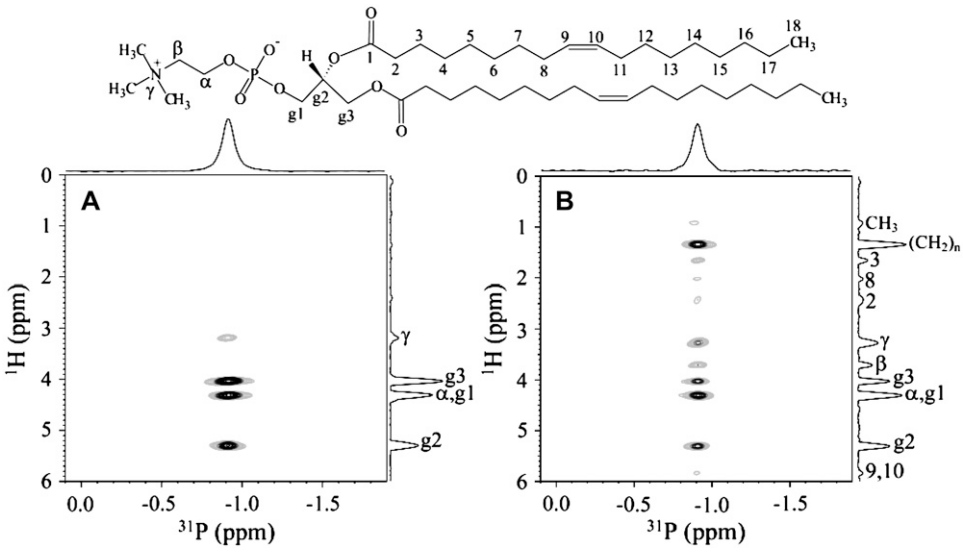

FIGURE 4 The two-dimensional ^{1}H-^{31}P CP dipolar HETCOR MAS NMR spectra for DOPC recorded at a sample temperature of 301 K with two different NOE mixing periods; (*A*) $\tau_m = 20$ μs and (*B*) $\tau_m = 500$ ms. The structure of DOPC with the nomenclature is depicted above the NMR spectra.

molecules due to membrane disorder. The choline Hγ protons do not cross-polarize to ^{31}P at the same contact time in SM, indicating that DOPC are more disordered than SM bilayers, or that these protons environments in SM are more dynamic. The other interesting difference between SM and DOPC is the significant ^{1}H-^{31}P correlation observed for $(CH_2)_n$ and C2′ in SM (Fig. 2 *B*) that is essentially not observed in the spectrum of DOPC (Fig. 4 *B*) for the same length mixing periods. Since the $(CH_2)_n$ interaction is intermolecular in origin, this strong correlation is consistent with the tighter chain packing of SM versus DOPC previously observed by ^{2}H NMR studies (15). For a 500-ms mixing period, ^{1}H-^{31}P correlations are observed for almost all environments (Fig. 4 *B*) consistent with rapid ^{1}H-^{1}H magnetization exchange resulting from lipid disorder as previously proposed (62,63). The one exception is that no correlation between H_2O and the ^{31}P of the headgroup is observed for mixing times between 1 and 500 ms (see Fig. 5 for a stack plot of the ^{1}H dimension through the ^{31}P DOPC resonance as a function of τ_m) in contrast with the SM results presented in Figs. 2 and 3. In addition, other PC lipids systems such as DMPC and DPPC displayed similar results to DOPC with no ^{1}H/^{31}P HETCOR correlation between H_2O and ^{31}P observed (data not shown). This again supports that the strong dipolar network observed between SM and H_2O arises from unique interactions at the sphingosine backbone.

^{1}H/^{13}C two-dimensional INEPT HETCOR of SM and DOPC bilayers

To further investigate these water-backbone interactions in SM, a series of two-dimensional ^{1}H-^{13}C INEPT HETCOR MAS NMR experiments were performed as shown in Fig. 6. By utilizing the INEPT component, the final ^{1}H-^{13}C transfer results from ^{1}H-^{13}C J couplings; this is such that, for the interpulse delays utilized, the final ^{13}C correlation results from directly bonded protons and does not arise from through space ^{1}H-^{13}C dipolar couplings. This is confirmed in Fig. 6 *A*, where only the expected direct one-bond C-H correlations are observed. Inclusion of a 50 ms ^{1}H-^{1}H NOE mixing period in this sequence (58) now allows correlations between different proton environments to be measured in the ^{13}C dimension (analogous to a ^{1}H-^{1}H relay experiment) as seen in Fig. 6 *B*. In this two-dimensional spectrum, multiple new correlation resonances are observed. We are particularly interested in the interactions with H_2O. The ^{13}C NMR spectrum along the ^{1}H chemical shift of H_2O ($\delta = +4.8$ ppm) is shown as the upper projection in Fig. 6 *B*. Correlations between H_2O and the protons on the C4, C5, C3, and C2/Cγ carbons are observed. The ^{13}C resonances of the C2/Cγ environment overlap, not allowing us to identify which interaction is occurring; but it assumed it is primarily with the C2 environment. Minor correlations between H_2O and the protons on the C1, Cα, and Cβ carbons were also detected. H_2O correlations with protons at other carbon environments were not observed. Similar two-dimensional ^{1}H-^{13}C INEPT experiments on DOPC with an equivalent 50-ms mixing time revealed no correlations between H_2O and any of the protons on that lipid system (results not shown). These results also support the argument that there is a unique H_2O environment associated with the sphingosine backbone in SM.

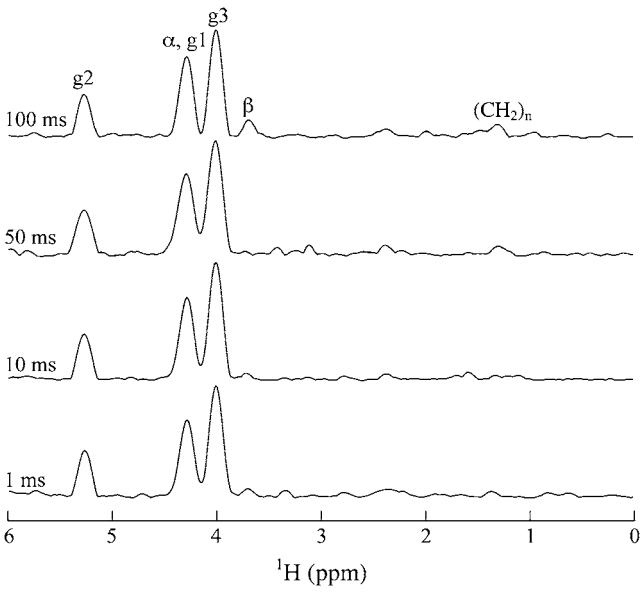

FIGURE 5 The ^{1}H projections from the two-dimensional ^{1}H-^{31}P CP dipolar HETCOR MAS NMR spectra for DOPC (Fig. 4) at increasing mixing periods' τ_m.

^{1}H/^{31}P two-dimensional dipolar HETCOR of SM/DOPC bilayers

The two-dimensional ^{1}H/^{31}P dipolar HETCOR spectrum for a 50:50 lipid mixture of SM and DOPC is shown in Fig. 7. For a short $\tau_m = 20$ μs mixing time, the ^{31}P resonances for SM ($\delta = -0.3$) and DOPC ($\delta = -0.9$) are clearly resolved. The 0.6 ppm increase in the chemical shift of SM has been attributed to hydrogen-bonding motifs that are not present in phosphatidylcholines (60,64). The ^{1}H dimension displays resonances resulting from protons that cross-polarize to the headgroup ^{31}P nuclei similar to the pure lipid samples (see Fig. 2 *A* and Fig. 4 *A*). The higher intensity of the DOPC spectrum compared to SM indicates an improved CP efficiency for DOPC at 1-ms contact time. This suggests that the ^{1}H-^{31}P dipolar coupling is smaller in SM than DOPC, in agreement with previous measurements of the ^{1}H-^{31}P dipolar coupling in similar SM and PC lipids (45). Measurements of the ^{31}P chemical shift anisotropy in SM/DOPC mixtures indicate similar headgroup dynamics in the liquid crystalline phase (33) pointing toward different ^{1}H-^{31}P distances and different headgroup configurations producing the changes in the dipolar coupling. When the spectrum is collected with $\tau_m = 500$ ms ^{1}H-^{1}H mixing period (Fig. 7 *B*), a significant H_2O resonance is observed for SM, while DOPC only dis-

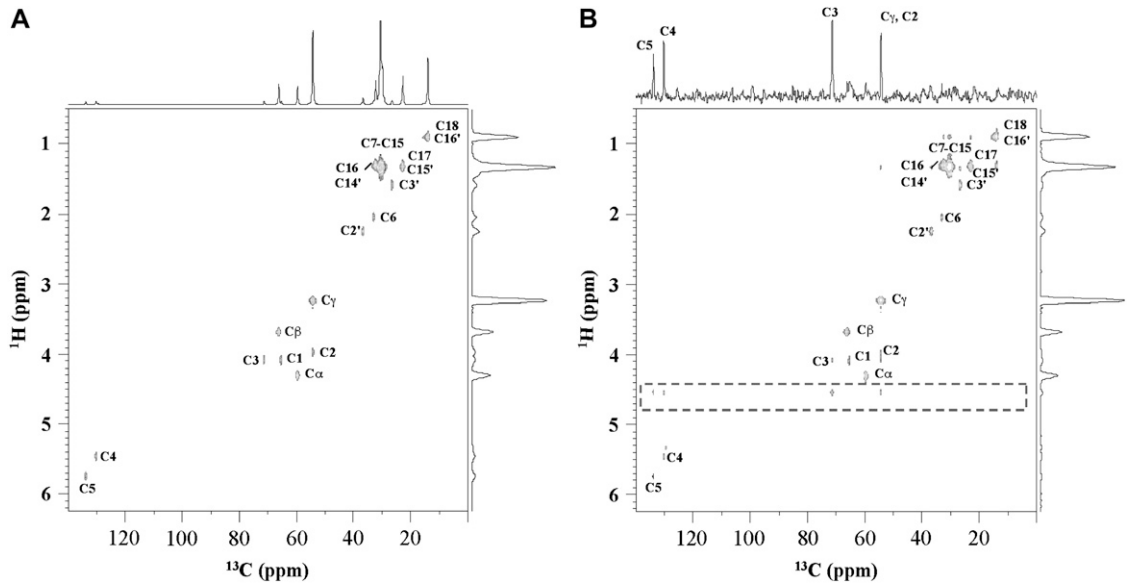

FIGURE 6 The two-dimensional ^{1}H-^{13}C INEPT HETCOR MAS NMR spectra for SM with (*A*) $\tau_m = 10\ \mu s$ ^{1}H-^{1}H NOE mixing period and a (*B*) $\tau_m = 50$ ms mixing period. The SM ^{1}H/^{13}C assignments are shown. The top ^{13}C projection in panel *B* is the slice along the H_2O $\delta(^{1}H) = +4.8$ ppm chemical shift.

plays a minor H_2O crosspeak. This shows that even in mixtures with DOPC, a significant interaction between SM and H_2O persists and DOPC has a minor but detectable interaction with H_2O. This is in contrast with the pure DOPC two-dimensional ^{1}H/^{31}P dipolar HETCOR spectrum, where no detectable interaction with H_2O was observed under similar conditions (see Fig. 5). This provides some evidence that H_2O may facilitate the interaction between neighboring lipids in mixtures with SM by forming water bridges as proposed previously (19).

DISCUSSION

It is thought that the H_2O contact detected when an NOE mixing period is included in the ^{1}H/^{31}P dipolar HETCOR and ^{1}H/^{13}C INEPT experiments presented here differs from the H_2O that was observed in previous ^{1}H/^{31}P HOESY studies of lipids (26). In the HOESY studies, an H_2O contact was detected in both PC and SM lipids in contrast with the dipolar HETCOR results presented here, where a H_2O contact is only observed in SM. This is due to the difference between the two NMR experiments utilized in the two studies. In the previous study, ^{1}H-^{31}P NOEs are detected, although, in this study, ^{1}H-^{1}H NOEs are detected indirectly by the final CP step to ^{31}P. It was concluded in the HOESY work that the contact observed is due to H_2O hydrogen-bonded to the phosphate group in close enough proximity to display a ^{1}H-^{31}P NOE contact. These H_2O molecules do not cross-polarize to ^{31}P (see Fig. 2 *A* and Fig. 4 *A*). This is probably due to a combination of rapid H_2O dynamics and long distances (weak dipolar coupling), resulting in poor ^{1}H-^{31}P CP efficiency. The H_2O correlations observed in this study (which are dipolar-coupled to Hα and H1 in SM but show no significant dipolar coupling to the headgroup or backbone protons of

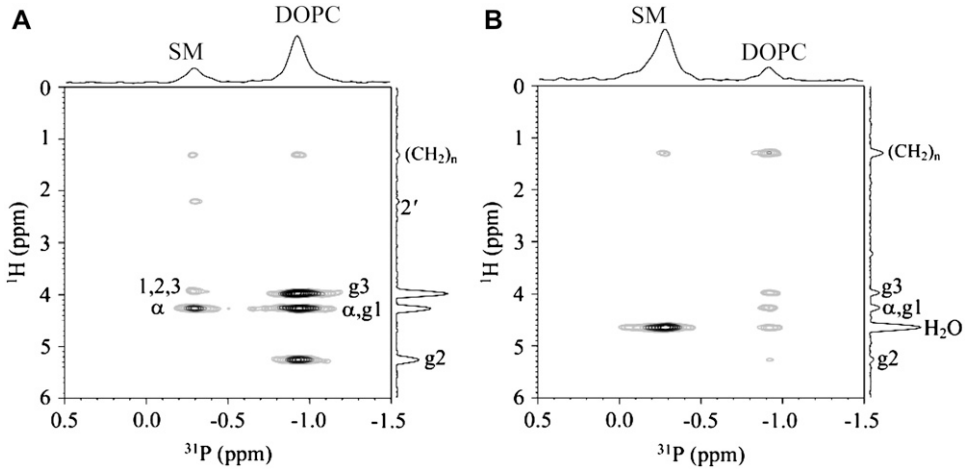

FIGURE 7 The two-dimensional ^{1}H-^{31}P CP dipolar HETCOR MAS NMR spectra for a 1:1 SM/DOPC mixture recorded at a sample temperature of 318 K with two different ^{1}H-^{1}H NOE mixing periods; (*A*) $\tau_m = 20\ \mu s$ and (*B*) $\tau_m = 500$ ms.

pure PC lipids) is believed to originate from H_2O that interacts at the backbone NH or OH groups. If the H_2O contact observed here was simply due to the ones bound to the phosphate group, a contact would be expected in the other PC lipids similar to the HOESY studies. Thus, in the SM system the H_2O contact must result from H_2O interactions at the SM backbone.

In a two-dimensional ^{1}H NOE spectroscopy (NOESY) NMR spectrum, crosspeaks arising from cross-relaxation correlations in the spin-diffusion or slow-tumbling limit ($\omega_0\tau_0 \gg 1$, negative NOE) will have the same sign as the autocorrelation diagonal (positive phase), and would be expected for both intra- and intermolecular lipid contacts, as well as water-lipid contacts where the water is closely associated with the lipid and has a lifetime $>\sim$1–10 ns. An example of these positive phase water/lipid correlations is seen in the ^{1}H NOESY spectrum of SM (see Supplementary Material, Data S1). Cross-relaxation correlations arising from rapid motion in the extreme narrowing limit will have a negative phase (positive NOE) as observed for small molecules, including water with short association lifetimes ($<$1 ns). The latter NOE effects (negative phase) have been reported previously in DOPC lipid systems (34), DMPC (Data S1), along with the careful characterization by Gawrisch et al. in a ^{1}H NOESY study on 1-palmitoyl-2-oleoyl-*sn*-glycero-3 phosphocholine (POPC) where a water/lipid lifetime of 100 ps was determined (65). Crosspeaks that arise from chemical exchange involving water will also have the same phase as the diagonal (positive phase), and are not readily distinguished from correlations produced from interactions in the spin-diffusion limit (66). Positive phase water/lipid correlation peaks have been reported in the NOESY spectrum of monomethyldioleoyl phosphatidylethanolamine and were attributed to either water contacts with long lifetimes or to the exchange process (34,61). A similar phase argument holds for the ^{1}H-^{31}P and ^{1}H-^{13}C dipolar HETCOR experiments presented in this article, since the magnetization exchange during the mixing period occurs via the same mechanism as the NOESY experiment.

In large biomolecules, chemical exchange between water and exchangeable protons followed by relay or transfer to nonexchangeable protons is a documented phenomena (67). These exchange crosspeaks will also have a positive phase in both the ^{1}H NOESY and dipolar HETCOR spectra, are not readily distinguished from the more direct cross-relaxation process, and in many instances may be the dominant process. Strong positive NOESY crosspeaks are clearly observed in the two-dimensional ^{1}H NOESY MAS NMR of SM (see Data S1), as well as the ^{1}H-^{31}P dipolar HETCOR (Fig. 2 and Fig. 7) and the ^{1}H-^{13}C INEPT HETCOR (Fig. 6) of SM and SM/DOPC. This is consistent with an exchange process involving the NH and/or the OH protons in the SM backbone. To determine if the positive phase water correlations result from an exchange process or are due to ^{1}H-^{1}H NOEs from water with a long ($>$1 ns) lipid association lifetime, two-dimensional ^{1}H-^{31}P dipolar HETCOR measurements were made as a function of τ_m and temperature. These results are presented in Fig. 8. Measurements were made in both the gel and liquid crystalline phases. In the gel phase, the water correlation buildup is rapid whereas, in the liquid crystalline phase, the rate constant is slower and decreases very slightly as the sample temperature is increased. In addition, there is an overall decrease in the normalized water peak intensity with increasing temperature.

The decrease in water correlation buildup rate with increasing temperature is the opposite of what would be expected for a relayed transfer due to water exchanging at an exchangeable proton environment at the SM backbone. It has been shown that, in the slow motion limit, an increase in the proton exchange rate results in positive NOE crosspeaks with an increased buildup rate (67). ^{2}H NMR studies (23) of SM have measured the OH exchange rate in a similar temperature range to the one in Fig. 8 where the exchange rate increased from $\sim$400 s^{-1} (312 K) to $\sim$1000 s^{-1} (328 K), consistent with these protons being in rapid exchange with the interlamellar waters in the liquid crystalline phase. If the observed water contact was dominated by this exchange mechanism, the water correlation buildup would be predicted to increase as the rate of exchange increases with temperature; clearly not what is observed (see Fig. 8).

The observed decrease in the buildup of the water resonance with temperature is consistent with what is typically reported for a direct cross-relaxation process in the slow motion limit. As detailed by Ernst et al. (68), in the slow motion regime the intensity of NOE correlations as a function of mixing time is proportional to the distance between the two

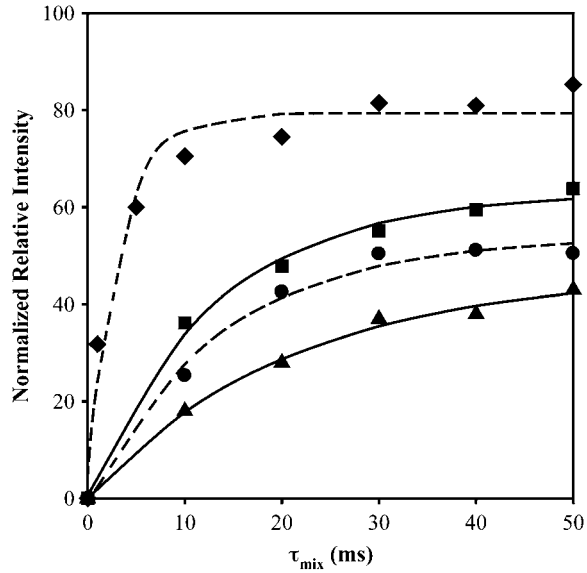

FIGURE 8 Normalized buildup curves for the H_2O contact extracted from the two-dimensional ^{1}H-^{31}P CP dipolar HETCOR MAS NMR spectra as a function of τ_m and temperature. NOE buildups were collected for SM in the gel phase, $T = 308$ K (♦) and three temperatures in the liquid crystalline phase, $T = 313$ K (■), 318 K (●), and 323 K (▲).

spins and the correlation time (τ_c) for reorientation of the internuclear vector as

$$I_{AB}(\tau_m) \propto \frac{\tau_c}{r_{AB}^6}\tau_m, \quad (1)$$

where r_{AB} is the distance between spins A and B. If we assume the ^{1}H-^{1}H distance remains reasonably constant, the observed decrease in the buildup rate of the water contact as a function of temperature can be attributed to the decrease in lipid and water correlation times with increasing temperature. This is further supported by the results presented in the gel phase, where the correlation times are expected to increase significantly compared to the liquid crystalline phase and as a result, a much faster buildup rate is observed (see Fig. 8). The temperature dependence of the NOE water contact presented here is similar to what has been observed in POPC and 1-stearoyl-2-oleoyl-*sn*-glycero-3-phophocholine where intermolecular contacts were detected between lipid-water and lipid-ethanol in the two systems, respectively (66,69). In those two studies, there were no exchangeable protons in the system and the decrease in NOE buildup was attributed to a decrease in τ_c with increasing temperature. It is therefore concluded, that the NOE water contact observed here in SM is not a result of an exchange process, but rather due to a strong hydrogen-bonded water environment at the sphingosine backbone with a long lipid-water association lifetime ($>$1 ns).

The same ^{2}H NMR study discussed above (23) was unable to detect NH exchange, in contrast with the OH site that displayed rapid exchange with water. This indicated that the NH is involved in strong hydrogen-bonding. Molecular dynamics (70) simulations also indicate that it is primarily the NH group that participates in intermolecular hydrogen-bonding in SM with a relatively high probability of those H-bonds being formed with water. Thus, we tentatively assign the water environment with a long lipid association lifetime observed here, to water molecules hydrogen-bonded at the sphingosine backbone, most likely at the NH site.

It should be noted that we were unable to detect any negative phase correlations involving water in the pure SM or DOPC dipolar HETCOR experiments, or in the HETCOR experiments of the SM/DOPC mixture (Figs. 2–7). There are a few possible reasons for this result. In the ^{31}P (or ^{13}C) detected NOE exchange experiments described in this article, the final CP (or INEPT) transfer involves magnetization arising from NOE exchange to these specific ^{1}H environments (the Hα, H1, H2, and H3 of SM), as well as the magnetization of these environments that did not undergo NOE exchange (essentially the diagonal intensity of the NOESY spectrum). This produces a dynamic range issue, since the observed NOESY diagonal intensities (positive phase) are typically 2–3 orders-of-magnitude larger than the small negative phase H_2O/lipid NOE correlations. In addition, the other lipid/lipid NOE exchanges (positive phase) are also commonly an order-of-magnitude larger than these H_2O/lipid NOE effects. This would suggest that any small negative phase H_2O/lipid NOE are being swamped by the larger positive phase correlations in the HETCOR experiments. Another factor that may contribute to not observing these negative phase H_2O/lipid NOE correlations is the diminished resolution in the F_1 dimension (128–256 points), giving rise to t_1 noise. This is why, in many NOESY analyses, the water correlations are extracted from the F_2 dimension where higher spectral resolution is obtained. This is not an option in the dipolar HETCOR experiments. The resolution in F_1 could also be improved by increasing the number of t_1 increments but, unfortunately, this would prove to be highly time-extensive for these types of dipolar HETCOR experiments.

These HETCOR results strongly support the presence of strong H_2O interactions at the backbone of SM. The detection of a H_2O contact between both SM and DOPC in a 50:50 mixture may also provide some evidence for the existence of bridging H_2O molecules in lipid mixtures containing SM. It will be interesting to use the techniques presented here to detect the presence or absence of this water-backbone interaction when cholesterol is incorporated in the bilayer and in more complex raft-forming lipid mixtures and will be the efforts of future research.

CONCLUSIONS

^{1}H/^{31}P dipolar HETCOR and ^{1}H/^{13}C INEPT HETCOR MAS NMR methods are useful for the study of intra- and intermolecular contacts in lipid mixtures when a mixing period is included in the pulse sequence to monitor ^{1}H-^{1}H NOEs. A specifically interesting result of this work is the detection of a strong interaction between H_2O and backbone protons in SM that is not observed in PC lipids. This could result from the unique hydrogen-bonding properties of the sphingosine backbone of SM. The lack of water contacts to the acyl chain of the lipid supports previous arguments that the water content in the hydrophobic core is very low. It is also interesting that a H_2O contact is observed in DOPC when it is in a 50:50 mixture with SM. This provides some evidence that bridging hydrogen-bonded water molecules are present between lipids in mixtures with SM. The presence of these H_2O species at the backbone is consistent with the low H_2O permeability in SM. These unique waters may also impact the membrane chemical potential and play a unique role in bilayer repulsion and cell fusion, as well as influence the targeting of amphiphilic peptides and proteins at the membrane surface.

It should be possible with future NMR experiments of this type to determine whether this unique water contact is indeed present at the NH moiety and if it exists in mixtures with cholesterol and in raft-forming systems containing SM. The NMR experiments with ^{31}P detection have the advantage over ^{1}H detected NOESY methods in that unique lipids can be resolved in mixtures. This is not always the case with ^{1}H detected NOESY experiments where the ^{1}H resonances of

lipids with different headgroups are typically not well resolved and thus, only single component lipid mixtures are typically studied.

SUPPLEMENTARY MATERIAL

To view all of the supplemental files associated with this article, visit www.biophysj.org.

Sandia is a multiprogram laboratory operated by Sandia Corporation, a Lockheed Martin Company, for the United States Department of Energy's National Nuclear Security Administration under Contract No. DE-AC04-94AL85000. This work was entirely supported by the Sandia Laboratory Directed Research and Development program.

REFERENCES

1. Barenholz, Y., and T. E. Thompson. 1980. Sphingomyelins in bilayers and biological membranes. *Biochim. Biophys. Acta*. 604:129–158.
2. Simons, K., and E. Ikonen. 1997. Functional rafts in cell membranes. *Nature*. 387:569–572.
3. Simons, K., and D. Toomre. 2000. Lipid rafts and signal transduction. *Nat. Rev. Mol. Cell Biol.* 1:31–39.
4. Anderson, R. G. W., and K. Jacobson. 2002. A role for lipid shells in targeting proteins to caveolae, rafts, and other lipid domains. *Science*. 296:1821–1825.
5. Ikonen, E. 2001. Roles of lipid rafts in membrane transport. *Curr. Opin. Cell Biol.* 13:470–477.
6. Brown, D. A., and E. London. 1998. Function of lipid rafts in biological membranes. *Annu. Rev. Cell Dev. Biol.* 14:111–136.
7. Baron, G. S., K. Wehrly, D. W. Dorward, B. Chesebro, and B. Caughey. 2002. Conversion of raft associated prion protein to the protease-resistant state requires insertion of PrP-res (PrP^{Sc}) into contiguous membranes. *EMBO J*. 21:1031–1040.
8. Kakio, A., S. Nishimoto, K. Yanagisawa, Y. Kozutsumi, and K. Matsuzaki. 2002. Interactions of amyloid β-protein with various gangliosides in raft-like membranes: importance of GM1 ganglioside-bound form as an endogenous seed for Alzheimer amyloid. *Biochemistry*. 41:7385–7390.
9. Puri, A., P. Hug, K. Jernigan, J. Barchi, H.-J. Kim, J. Hamilton, J. Wiels, G. J. Murray, R. O. Brady, and R. Blumenthal. 1998. The neutral glycosphingolipid globotriaosylceramide promotes fusion mediated by a CD4-dependent CXCR4-utilizing HIV type 1 envelope glycoprotein. *Proc. Natl. Acad. Sci. USA*. 95:14435–14440.
10. Mañes, S., G. del Real, R. A. Lacalle, P. Lucas, and C. Gómez-Moutón. 2000. Membrane raft microdomains mediate lateral assemblies required for HIV-1 infection. *EMBO Rep*. 1:190–196.
11. Liao, Z., L. M. Cimakasky, R. Hampton, D. H. Nguyen, and J. E. K. Hildreth. 2001. Lipid rafts and HIV pathogenesis: host membrane cholesterol is required for infection by HIV type 1. *AIDS Res. Hum. Retroviruses*. 17:1009–1019.
12. Maxfield, F. R., and I. Tabas. 2005. Role of cholesterol and lipid organization in disease. *Nature*. 438:612–621.
13. van Duyl, B. Y., D. Ganchev, V. Chupin, B. de Kruijff, and J. A. Killian. 2003. Sphingomyelin is much more effective than saturated phosphatidylcholine in excluding unsaturated phosphatidylcholine from domains formed with cholesterol. *FEBS Lett*. 547:101–106.
14. Barenholz, Y., and T. E. Thompson. 1999. Sphingomyelin: biophysical aspects. *Chem. Phys. Lipids*. 102:29–34.
15. Mehnert, T., K. Jacob, R. Bittman, and K. Beyer. 2006. Structure and lipid interaction of *n*-palmitoylsphingomyelin in bilayer membranes as revealed by ^{2}H-NMR spectroscopy. *Biophys. J*. 90:939–946.
16. Huang, J., and G. W. Feigenson. 1999. A microscopic interaction model of maximum solubility of cholesterol in lipid bilayers. *Biophys. J*. 76:2142–2157.
17. Huang, J., J. T. Buboltz, and G. W. Feigenson. 1999. Maximum solubility of cholesterol in phosphatidylcholine and phosphatidylethanolamine bilayers. *Biochim. Biophys. Acta*. 1417:89–100.
18. Parker, A., K. Miles, K. H. Cheng, and J. Huang. 2004. Lateral distribution of cholesterol in dioleoylphosphatidylcholine lipid bilayers: cholesterol-phospholipid interactions at high cholesterol limit. *Biophys. J*. 86:1532–1544.
19. Talbott, C. M., I. Vorobyov, D. Borchman, K. G. Taylor, D. B. DuPré, and M. C. Yappert. 2000. Conformational studies of sphingolipids by NMR spectroscopy. II Sphingomyelin. *Biochim. Biophys. Acta*. 1467: 326–337.
20. Lamba, O. P., D. Borchman, S. K. Sinha, S. Lal, M. C. Yappert, and M. F. Lou. 1991. Structure and molecular conformation of anhydrous and of aqueous sphingomyelin bilayers determined by infrared and Raman spectroscopy. *J. Mol. Struct*. 248:1–24.
21. Villalain, J., A. Ortiz, and J. C. Gomez-Fernandez. 1988. Molecular interactions between sphingomyelin and phosphatidylcholine in phospholipid vesicles. *Biochim. Biophys. Acta. Biomembranes*. 941: 55–62.
22. Bruzik, K. S. 1988. Conformation of the polar headgroup of sphingomyelin and its analogues. *Biochim. Biophys. Acta. Biomembranes*. 939:315–326.
23. Steinbauer, B., T. Mehnert, and K. Beyer. 2003. Hydration and lateral organization in phospholipid bilayers containing sphingomyelin: a ^{2}H NMR study. *Biophys. J*. 85:1013–1024.
24. Bonev, B. B., W. C. Chan, B. W. Bycroft, G. C. K. Roberts, and A. Watts. 2000. Interaction of the lantibiotic nisin with mixed lipid bilayers: a ^{31}P and ^{2}H NMR study. *Biochemistry*. 39:11425–11433.
25. Guo, W., V. Kurze, T. Huber, N. H. Afdhal, K. Beyer, and J. A. Hamilton. 2002. A solid-state NMR study of phospholipid-cholesterol interactions: sphingomyelin-cholesterol binary systems. *Biophys. J*. 83:1465–1478.
26. Warschawski, D. E., P. Fellmann, and P. F. Devaux. 1996. High-resolution ^{31}P-^{1}H two-dimensional nuclear magnetic resonance spectra of unsonicated lipid mixtures spinning at the magic-angle. *Eur. Biophys. J*. 25:131–137.
27. Spooner, P. J. R., and A. Watts. 1992. Cytochrome *c* interactions with cardiolipin in bilayers: a multinuclear magic-angle spinning NMR study. *Biochemistry*. 31:10129–10138.
28. Pinheiro, T. J. T., and A. Watts. 1994. Resolution of individual lipids in mixed phospholipid membranes and specific lipid-cytochrome *c* interactions by magic-angle spinning solid-state phosphorous-31 NMR. *Biochemistry*. 33:2459–2467.
29. Bonev, B., A. Watts, M. Bokvist, and G. Gröbner. 2001. Electrostatic peptide-lipid interactions of amyloid-β peptide pentalysine with membrane surfaces monitored by ^{31}P MAS NMR. *Phys. Chem. Chem. Phys.* 3:2904–2910.
30. Bokvist, M., F. Lindström, A. Watts, and G. Gröbner. 2004. Two types of Alzheimer's β-amyloid (1–40) peptide membrane interactions: aggregation preventing transmembrane anchoring versus accelerated surface fibril formation. *J. Mol. Biol.* 335:1039–1049.
31. Lindström, F., P. T. F. Williamson, and G. Gröbner. 2005. Molecular insight into the electrostatic membrane surface potential by ^{14}N/^{31}P MAS NMR spectroscopy: nociceptin-lipid association. *J. Am. Chem. Soc*. 127:6610–6616.
32. Costello, A. L., and T. M. Alam. 2008. Using ^{31}P MAS NMR to monitor a gel phase thermal disorder transition in sphingomyelin/cholesterol bilayers. *Biochim. Biophys. Acta*. 1778:97–104.
33. Holland, G. P., S. K. McIntyre, and T. M. Alam. 2006. Distinguishing individual lipid headgroup mobility and phase transitions in raft-forming lipid mixtures with ^{31}P MAS NMR. *Biophys. J*. 90:1–13.
34. Zhou, Z., B. G. Sayer, D. W. Hughes, R. E. Stark, and R. M. Epand. 1999. Studies of phospholipid hydration by high-resolution magic-angle-spinning nuclear magnetic resonance. *Biophys. J*. 76:387–399.

35. Yeagle, P. L., W. C. Hutton, C.-H. Huang, and R. B. Martin. 1975. Headgroup conformation and lipid-cholesterol association in phosphatidylcholine vesicles: a $^{31}P\{^{1}H\}$ nuclear Overhauser effect study. *Proc. Natl. Acad. Sci. USA.* 72:3477–3481.

36. Yeagle, P. L., W. C. Hutton, C.-H. Huang, and R. B. Martin. 1976. Structure in the polar head region of phospholipid bilayers: a $^{31}P\{^{1}H\}$ nuclear Overhauser effect study. *Biochemistry.* 15:2121–2124.

37. Burns, R. A., R. E. Stark, D. A. Vidusek, and M. F. Roberts. 1983. Dependence of phosphatidylcholine phosphorous-31 relaxation times and $^{31}P\{^{1}H\}$ nuclear Overhauser effect distribution on aggregate structure. *Biochemistry.* 22:5084–5090.

38. Shibata, T., J. Uzawa, and Y. Sugiura. 1983. Selective $^{31}P\{^{1}H\}$ nuclear Overhauser effect study on the polar headgroup conformation of phospholipids in micelles in organic solvents. *Chem. Phys. Lipids.* 33: 1–10.

39. Milburn, M. P., and K. R. Jeffrey. 1990. Dynamics of the phosphate group in phospholipid bilayers a ^{31}P-^{1}H transient Overhauser effect study. *Biophys. J.* 58:187–194.

40. Tauskela, J. S., and M. Thompson. 1992. A ^{31}P-NMR spin-lattice relaxation and $^{31}P\{^{1}H\}$ nuclear Overhauser effect study of sonicated small unilamellar phosphatidylcholine vesicles. *Biochim. Biophys. Acta.* 1104:137–146.

41. Warschawski, D. E., and P. F. Devaux. 2000. Polarization transfer in lipid membranes. *J. Magn. Reson.* 145:367–372.

42. Guo, W., and J. A. Hamilton. 1995. A multinuclear solid-state NMR study of phospholipid-cholesterol interactions. Dipalmitoylphosphatidylcholine-cholesterol binary system. *Biochemistry.* 34:14174–14184.

43. Bruzik, K. S., B. Sobon, and G. M. Salamonczyk. 1990. Nuclear magnetic resonance study of sphingomyelin bilayers. *Biochemistry.* 29:4017–4021.

44. Warschawski, D. E., and P. F. Devaux. 2005. ^{1}H-^{13}C polarization transfer in membranes: a tool for probing lipid dynamics and the effect of cholesterol. *J. Magn. Reson.* 177:166–171.

45. Hong, M., K. Schmidt-Rohr, and D. Nanz. 1995. Study of phospholipid structure by ^{1}H, ^{13}C, and ^{31}P dipolar couplings from two-dimensional NMR. *Biophys. J.* 69:1939–1950.

46. Dvinskikh, S. V., and D. Sandström. 2005. Efficient solid-state NMR methods for measuring heteronuclear dipolar couplings in unoriented lipid membrane systems. *Phys. Chem. Chem. Phys.* 7:607–613.

47. Holland, G. P., and T. M. Alam. 2006. Multi-dimensional ^{1}H-^{13}C HETCOR and FSLG-HETCOR NMR study of sphingomyelin bilayers containing cholesterol in the gel and liquid crystalline states. *J. Magn. Reson.* 181:316–326.

48. Akutsu, H., and Y. Kyogoku. 1984. Phase transitions of phosphatidylcholine bilayers as revealed by cross-polarization efficiency of P-31 NMR. *Biochim. Biophys. Acta.* 774:293–295.

49. Frye, J., A. D. Albert, B. S. Selinsky, and P. L. Yeagle. 1985. Cross polarization P-31 nuclear magnetic resonance of phospholipids. *Biophys. J.* 48:547–552.

50. Odahara, T., H. Akutsu, and Y. Kyogoku. 1990. Direct observation of the phase behavior of the lipid bilayers of phage PM2 and the intact host cells by ^{1}H-^{31}P cross-polarization NMR. *Biochemistry.* 29:5968–5974.

51. Mitrakos, P., and P. M. McDonald. 2000. Nucleotide chain length and the morphology of complexes with cationic amphiphiles: ^{31}P-NMR observations. *Biochim. Biophys. Acta.* 1463:355–373.

52. Hanamura, T., N. Asakawa, Y. Inoue, and M. Sakurai. 1998. A solid-state ^{31}P NMR study of the interaction between trehalose and DPPC bilayer. *Chem. Lett.* (*Jpn.*). 8:713–714.

53. Traïkia, M., D. E. Warschawski, M. Recouvreur, J. Cartaud, and P. F. Devaux. 2000. Formation of unilamellar vesicles by repetitive freeze-thaw cycles: characterization by electron microscopy and ^{31}P-nuclear magnetic resonance. *Eur. Biophys. J.* 29:184–195.

54. Dvinskikh, S. V., V. Castro, and D. Sandström. 2004. Heating caused by radio frequency irradiation and sample rotation in ^{13}C magic angle spinning NMR studies of lipid membranes. *Magn. Reson. Chem.* 42:875–881.

55. Bennett, A. E., C. M. Rienstra, M. Auger, K. V. Lakshmi, and R. G. Griffin. 1995. Heteronuclear decoupling in rotating solids. *J. Chem. Phys.* 103:6951–6958.

56. Metz, G., X. L. Wu, and S. O. Smith. 1994. Ramped-amplitude cross polarization in magic-angle-spinning NMR. *J. Magn. Reson. A.* 110: 219–227.

57. Schmidt-Rohr, K., J. Clauss, and H. W. Spiess. 1992. Correlation of structure, mobility, and morphological information in heterogeneous polymer materials by two-dimensional wideline-separation NMR spectroscopy. *Macromolecules.* 25:3273–3277.

58. Alam, T. M., and G. P. Holland. 2006. ^{1}H-^{13}C INEPT MAS NMR correlation experiments with ^{1}H-^{1}H mediated magnetization exchange to probe organization in lipid biomembranes. *J. Magn. Reson.* 180: 210–221.

59. Chiu, S. W., S. Vasudevan, E. Jakobsson, R. J. Mashl, and H. L. Scott. 2003. Structure of sphingomyelin bilayers: a simulation study. *Biophys. J.* 85:3624–3635.

60. Schmidt, C. F., Y. Barenholz, and T. E. Thompson. 1977. A nuclear magnetic resonance study of sphingomyelin in bilayer systems. *Biochemistry.* 16:2649–2656.

61. Chen, J.-Z., and R. E. Stark. 1996. Evaluating spin diffusion in MAS-NOESY spectra of phospholipid multibilayers. *Solid State Nucl. Magn. Reson.* 7:239–246.

62. Huster, D., K. Arnold, and K. Gawrisch. 1999. Investigation of lipid organization in biological membranes by two-dimensional nuclear Overhauser enhancement spectroscopy. *J. Phys. Chem. B.* 103:243–251.

63. Huster, D., and K. Gawrisch. 1999. NOESY NMR crosspeaks between lipid headgroups and hydrocarbon chains: spin diffusion or molecular disorder. *J. Am. Chem. Soc.* 121:1992–1993.

64. Henderson, T. O., T. Glonek, and T. C. Myers. 1974. Phosphorous-31 nuclear magnetic resonance spectroscopy of phospholipids. *Biochemistry.* 13:623–628.

65. Gawrisch, K., H. C. Gaede, M. Mihailescu, and S. H. White. 2007. Hydration of POPC bilayers studied by ^{1}H-PFG-MAS-NOESY and neutron diffraction. *Eur. Biophys. J.* 36:281–291.

66. Croasmun, W. R., and R. M. K. Carlson. 1994. Two-Dimensional NMR Spectroscopy. John Wiley and Sons, New York.

67. van de Ven, F. J. M., H. G. J. M. Janssen, A. Gräslund, and C. W. Hilbers. 1988. Chemical relayed nuclear Overhauser effects. Connectivities between resonance of nonexchangeable protons and water. *J. Magn. Reson.* 79:221–235.

68. Ernst, R. R., G. Bodenhausen, and A. Wokaun. 2003. Principles of Nuclear Magnetic Resonance in One and Two Dimensions. Oxford University Press, New York.

69. Holte, L., and K. Gawrisch. 1997. Determining ethanol distribution in phospholipid multilayers with MAS-NOESY spectra. *Biochemistry.* 36:4669–4674.

70. Mombelli, E., R. Morris, W. Taylor, and F. Fraternali. 2003. Hydrogen-bonding propensities of sphingomyelin in solution and in a bilayer assembly: a molecular dynamics study. *Biophys. J.* 84:1507–1517.